

See discussions, stats, and author profiles for this publication at: <https://www.researchgate.net/publication/280492540>

# Solvent-Dependent Structural Variation of Zinc(II) Coordination Polymers and Their Catalytic Activity in the Knoevenagel Condensation Reaction

ARTICLE in CRYSTAL GROWTH & DESIGN · JULY 2015

Impact Factor: 4.89 · DOI: 10.1021/acs.cgd.5b00948

---

READS

30

## 5 AUTHORS, INCLUDING:



M Fátima C Guedes da Silva

University of Lisbon

260 PUBLICATIONS 4,155 CITATIONS

[SEE PROFILE](#)



Susanta Hazra

Technical University of Lisbon

38 PUBLICATIONS 514 CITATIONS

[SEE PROFILE](#)

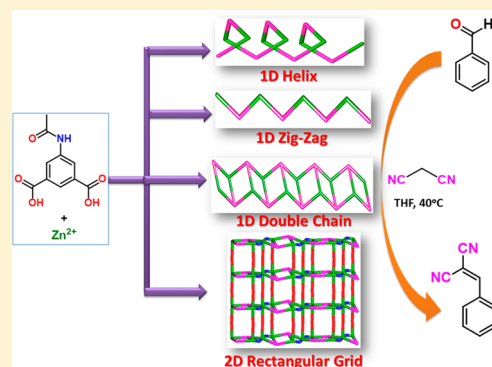
# Solvent-Dependent Structural Variation of Zinc(II) Coordination Polymers and Their Catalytic Activity in the Knoevenagel Condensation Reaction

Anirban Karmakar,\* Guilherme M. D. M. Rúbio, M. Fátima C. Guedes da Silva,\* Susanta Hazra, and Armando J. L. Pombeiro\*

Centro de Química Estrutural, Instituto Superior Técnico, Universidade de Lisboa, Av. Rovisco Pais, 1049–001, Lisbon, Portugal

 Supporting Information

**ABSTRACT:** The novel self-assembled zinc(II) coordination polymers  $[Zn(L)(H_2O)_2]_n$  (**1**),  $[Zn(L)(H_2O)_2]_n \cdot n(\text{formamide})$  (**2**),  $[Zn(L)(H_2O)_2]_n \cdot n(N\text{-methylformamide})$  (**3**),  $[Zn(L)(H_2O)(\text{formamide})]_n$  (**4**), and  $[Zn_3(L)_2(\text{formate})_2(4,4'\text{-bipyridine})_3]_n \cdot 2n(\text{DMF}) \cdot 2n(H_2O)$  (**5**) ( $L = 5\text{-acetamidoisophthalate}$ ) have been synthesized and characterized by elemental microanalysis, infrared spectroscopy, thermogravimetric analysis, and X-ray single crystal X-ray diffraction. **1**, **2**, and **3** are one-dimensional (1D) coordination polymers that crystallize in monoclinic  $P2_1$ , monoclinic  $P2_1/m$ , and triclinic  $P\bar{I}$  systems, respectively, and are pseudo-polymorphic supramolecular isomers with **1** having a helical arrangement, and **2** and **3** exhibiting zigzag type structures containing different guest molecules. Compound **4** crystallizes in the triclinic  $P\bar{I}$  space group and is a 1D coordination polymer that exhibits fused 8-membered and 16-membered dimetallic rings. Compound **5** features a two-dimensional network type polymer with trimetallic cores. Compounds **1**–**5** expand to three-dimensional by means of H-bond interactions. These coordination polymers act as effective heterogeneous catalysts, under mild conditions, for the Knoevenagel condensation reaction of different aldehydes with an active methylene compound (malononitrile) and can be recycled without losing activity.



## INTRODUCTION

Coordination polymers represent a class of materials that can be constructed by assembly of metal cations or their clusters as nodes and, usually, anionic organic ligands as linkers.<sup>1–11</sup> Their attractive architectures and topological networks account for their wide application in gas storage,<sup>12–15</sup> separation,<sup>16</sup> catalysis (see below), drug delivery,<sup>17,18</sup> and embedding of nanoparticles.<sup>19</sup> Because of various coordination modes they can be adjusted to satisfy the requirements of particular structural motifs. However, identical chemical components may produce more than one superstructure, known as supramolecular isomers.

Supramolecular isomers involve network structures that have identical chemical compositions but differ in their structures.<sup>20–23</sup> Pseudopolymorphic supramolecular isomers concern identical frameworks that contain different counterions, solvents, or guest molecules.<sup>20,22</sup> Similar to polymorphism, this phenomena results when different but energetically similar packing interactions can operate during crystallization; induction by variation of temperature, solvent, conformation of the ligand, etc., has been well established.<sup>24–27</sup> A variety of examples of supramolecular isomerism in coordination polymers has been reported,<sup>28–32</sup> and this study is important not only in producing novel materials with interesting

properties but also in developing a fundamental understanding of the factors influencing crystal growth.

Many isomeric zinc(II) imidazolates featuring zeolite-like topologies have been formed by using template strategies.<sup>21</sup> Two Zn(II) based two-dimensional (2D) metal organic frameworks have recently been reported,<sup>29</sup> which are pseudo-supramolecular isomeric pairs, and two heterometallic coordination polymers<sup>32</sup> are good examples of pseudo-polymorphic supramolecular isomers. A number of coordination polymers or metal organic frameworks have been reported as supramolecular isomers, several being based on the coexistence of different guest molecules.<sup>24–32</sup>

Coordination polymers have recently been applied in heterogeneous catalysis<sup>33–38</sup> and as catalysts for several organic reactions,<sup>39–44</sup> e.g., alkylation of aromatics,<sup>45</sup> carbonyl-ene and Diels–Alder reaction,<sup>46</sup> cyanotrimethylsililation,<sup>47</sup> isomerization of  $\alpha$ -pinene oxide,<sup>48</sup> and the Mukaiyama–aldol reaction.<sup>49</sup> Recently, we have reported various coordination polymers which are catalytically active for the oxidation of alkanes, alcohols, or olefins.<sup>50–61</sup> Acidic and basic polymers can exhibit high catalytic activity in condensation reactions such as the Pechmann,<sup>62</sup> Knoevenagel,<sup>63–76</sup> and Prins reactions.<sup>77</sup> Coordi-

Received: February 3, 2015



nation polymers can work as catalysts through two different components, viz. the metal ions, which either provide the coordinatively unsaturated nodes and/or form the active metal sites integrated into the linker ligand, and the ligands. Depending on the nature of the ligands and binding metal ions, coordination polymers can act as Lewis bases or acids in the catalytic medium.

Recently, we have been focusing on the rational designing of various types of coordination polymers and discrete complexes using amido carboxylate ligands and different transition metal ions and their catalytic activity in various organic transformations, namely, the Henry reaction.<sup>78,79</sup> The amido carboxylate ligands are known to form interesting polymeric frameworks with metal ions.<sup>78,79</sup> Besides, the presence of carboxylate groups allows slight conformational changes for the potential assembly of different network architectures.

Thus, the two main objectives of the current work are as follows: (i) to synthesize Zn(II)-coordination polymers by using 5-acetamidoisophthalic acid linkers in presence or absence of auxiliary ligands, under various hydrothermal conditions; (ii) to apply the synthesized coordination polymers as heterogeneous catalysts for the Knoevenagel condensation reaction of different aldehydes with an active methylene compound.

Hence, we now report the synthesis of the novel 5-acetamidoisophthalic acid ( $\text{H}_2\text{L}$ ) species which is then applied to the preparation, under hydrothermal conditions, of new Zn(II)-coordination polymers. The strategy successfully yielded the polymeric materials  $[\text{Zn}(\text{L})(\text{H}_2\text{O})_2]_n$  (**1**),  $[\text{Zn}(\text{L})(\text{H}_2\text{O})_2]_n \cdot n(\text{formamide})$  (**2**),  $[\text{Zn}(\text{L})(\text{H}_2\text{O})_2]_n \cdot n(\text{N-methylformamide})$  (**3**),  $[\text{Zn}(\text{L})(\text{H}_2\text{O})(\text{formamide})]_n$  (**4**), and  $[\text{Zn}_3(\text{L})_2(4,4'\text{-bipyridine})_3]_n \cdot 2n(\text{DMF}) \cdot 2n(\text{H}_2\text{O})$  (**5**). The obtained frameworks act as heterogeneous catalysts in the Knoevenagel condensation reaction of malononitrile with various aldehydes.

## ■ EXPERIMENTAL SECTION

The synthetic work was performed in air. All the chemicals were obtained from commercial sources and used as received. The infrared spectra (4000–400  $\text{cm}^{-1}$ ) were recorded on a Bruker Vertex 70 instrument in KBr pellets, abbreviations: s = strong, m = medium, w = weak, bs = broad and strong, mb = medium and broad. The  $^1\text{H}$  and  $^{13}\text{C}$  NMR spectra were recorded at ambient temperature on a Bruker Avance II + 300 (UltraShieldMagnet) spectrometer operating at 300.130 and 75.468 MHz for proton and carbon-13, respectively. The chemical shifts are reported in ppm using tetramethylsilane as the internal reference, abbreviations: s = singlet, d = doublet, t = triplet, q = quartet. Carbon, hydrogen, and nitrogen elemental analyses were carried out by the Microanalytical Service of the Instituto Superior Técnico. Electrospray mass spectra (ESI-MS) were run with an ion-trap instrument (Varian 500-MS LC Ion Trap mass spectrometer) equipped with an electrospray ion source. For electrospray ionization, the drying gas and flow rate were optimized according to the particular sample with a 35 p.s.i. nebulizer pressure. Scanning was performed from  $m/z$  100 to 1200 in methanol solution. The compounds were observed in the positive mode (capillary voltage = 80–105 V). Thermal properties were analyzed with a PerkinElmer Instrument system (STA6000) at a heating rate of  $2\text{ }^\circ\text{C min}^{-1}$  under a dinitrogen atmosphere. Powder X-ray diffraction (PXRD) was conducted in a D8 Advance Bruker AXS (Bragg–Brentano geometry) theta-2theta diffractometer, with copper radiation ( $\text{Cu K}\alpha$ ,  $\lambda = 1.5406\text{ \AA}$ ) and a secondary monochromator, operated at 40 kV and 40 mA. Flat plate configuration was used, and the typical data collection range was between  $5^\circ$  and  $40^\circ$ .

**Synthesis of 5-Acetamidoisophthalic acid ( $\text{H}_2\text{L}$ ).** A 1.81 g (10 mmol) portion of 5-aminoisophthalic acid was dissolved in 20 mL of acetic anhydride, and the reaction mixture was refluxed for 4 h at 80

$^\circ\text{C}$ , after which 20 mL of water was added and the solution was further heated until boiling. After cooling, the obtained white solid product of 5-acetamidoisophthalic acid ( $\text{H}_2\text{L}$ ) was filtered off and washed with water until total removal of acetic acid. Yield: 85% (1.54 g).

FT-IR (KBr,  $\text{cm}^{-1}$ ): 3546 (s), 3451(s), 3130(mb), 1723(s), 1673(s), 1616(s), 1583(s), 1459(m), 1407(m), 1372(w), 1338(m), 1308(s), 1255(s), 1208(s), 1130(w), 1109(w), 1031(m), 1001(w), 989(w), 924(s), 806(s), 782(m), 755(s), 676(s), 608(w), 587(w), 542(w), 505(s).  $^1\text{H}$  NMR (DMSO- $d_6$ ): 10.29 (1H, s, -NH), 8.38 (2H, s, Ar-H), 8.13 (1H, s, Ar-H), 2.0 (3H, s, -CH<sub>3</sub>).  $^{13}\text{C}$  NMR (DMSO- $d_6$ ): 169.5, 166.9, 140.2, 132.0, 124.8, 123.8, 24.3. MS (ESI):  $m/z$ : 246.0 [M + Na]<sup>+</sup>.

**Synthesis of 1.** A mixture of  $\text{Zn}(\text{NO}_3)_2 \cdot 6\text{H}_2\text{O}$  (29 mg, 0.10 mmol) and  $\text{H}_2\text{L}$  (22 mg, 0.10 mmol) was dissolved in 1 mL of DMF and methanol (1:1). The resulting mixture was sealed in an 8 mL glass vessel and heated at 75  $^\circ\text{C}$  for 48 h. Subsequent gradual cooling to room temperature ( $0.2\text{ }^\circ\text{C min}^{-1}$ ) afforded colorless crystals of **1**. Yield: 54% (based on Zn). Anal. Calcd for  $\text{C}_{10}\text{H}_{11}\text{NO}_7\text{Zn}$  ( $M = 322.59$ ): C, 37.23; H, 3.44; N, 4.34; Found: C, 36.02; H, 3.65; N, 4.02. FT-IR (KBr,  $\text{cm}^{-1}$ ): 3351 (bs), 1680 (s), 1634 (s), 1562 (s), 1420 (m), 1364 (s), 1326 (m), 1282 (m), 1238 (m), 1192 (w), 1103 (m), 1031 (m), 987 (w), 952 (m), 815 (s), 772 (s), 737(m), 538 (w), 460 (m).

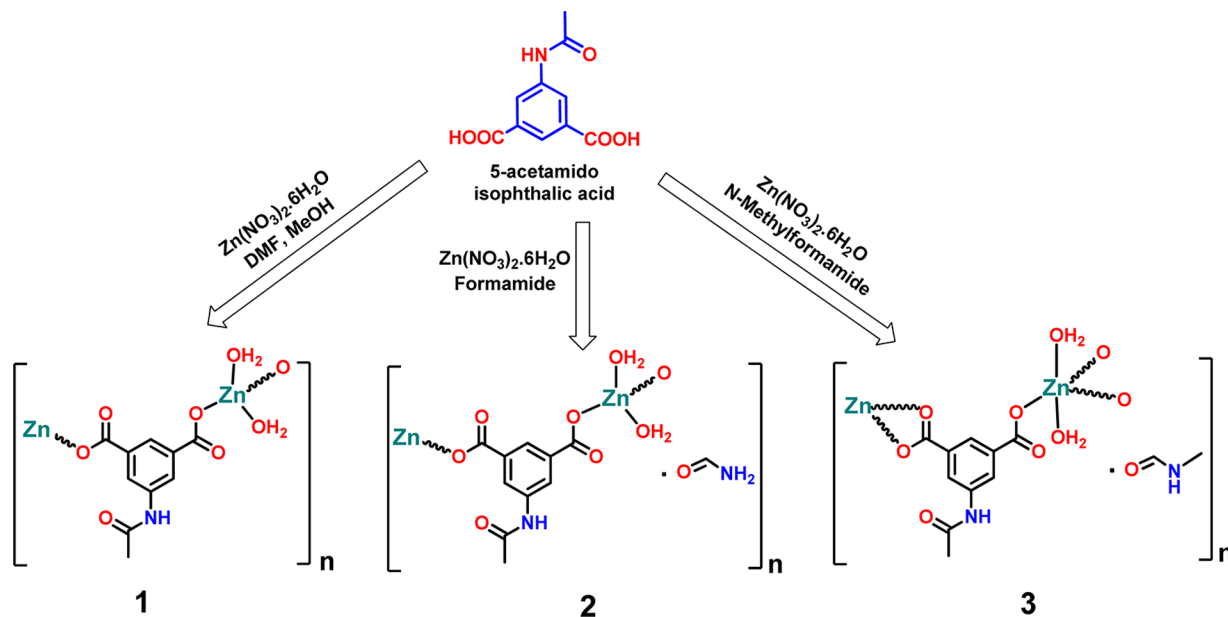
**Synthesis of 2.**  $\text{Zn}(\text{NO}_3)_2 \cdot 6\text{H}_2\text{O}$  (29 mg, 0.10 mmol) and  $\text{H}_2\text{L}$  (22 mg, 0.10 mmol) were dissolved in 1 mL of formamide, sealed in a capped glass vessel, and heated to 75  $^\circ\text{C}$  for 48 h. Subsequent gradual cooling to room temperature ( $0.2\text{ }^\circ\text{C min}^{-1}$ ) afforded colorless crystals of **2** in ca. 77% yield (based on Zn). Anal. Calcd for  $\text{C}_{11}\text{H}_{14}\text{N}_2\text{O}_8\text{Zn}$  ( $M = 367.63$ ): C, 35.94; H, 3.84; N, 7.62; Found: C, 36.11; H, 4.01; N, 7.45. FT-IR (KBr,  $\text{cm}^{-1}$ ): 3300 (bs), 2882 (w), 1679 (s), 1619 (s), 1580 (m), 1489 (s), 1451 (s), 1424 (m), 1352 (m), 1283 (m), 1221 (m), 1106 (w), 1069 (m), 1045 (m), 915 (w), 814 (s), 777 (s), 730 (m), 642 (m), 620 (m), 531 (m).

**Synthesis of 3.** A mixture of  $\text{Zn}(\text{NO}_3)_2 \cdot 6\text{H}_2\text{O}$  (29 mg, 0.10 mmol) and  $\text{H}_2\text{L}$  (22 mg, 0.10 mmol) was dissolved in 1 mL *N*-methylformamide. The resulting mixture was sealed in an 8 mL glass vessel and heated at 75  $^\circ\text{C}$  for 48 h. It was subsequently cooled to room temperature ( $0.2\text{ }^\circ\text{C min}^{-1}$ ), affording plate-like colorless crystals of **3**. Yield: 68% (based on Zn). Anal. Calcd for  $\text{C}_{12}\text{H}_{16}\text{N}_2\text{O}_8\text{Zn}$  ( $M = 381.66$ ): C, 37.77; H, 4.23; N, 7.34. Found: C, 37.53; H, 3.92; N, 7.10. FT-IR (KBr,  $\text{cm}^{-1}$ ): 3367 (bs), 2883 (w), 1683 (s), 1613 (s), 1580 (m), 1560 (m), 1490 (s), 1417 (m), 1390 (s), 1347 (s), 1275 (w), 1216 (w), 1100 (w), 1072 (m), 1032 (m), 809 (s), 782 (s), 725 (s), 642 (m), 531 (m).

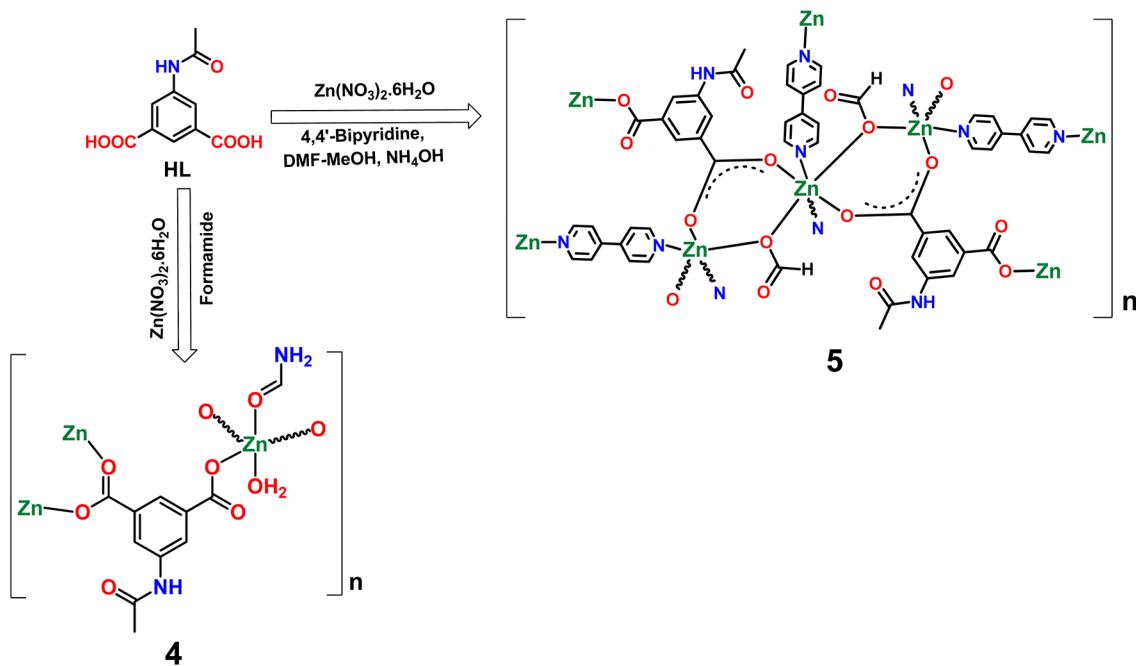
**Synthesis of 4.** A mixture of  $\text{Zn}(\text{NO}_3)_2 \cdot 6\text{H}_2\text{O}$  (58 mg, 0.20 mmol) and  $\text{H}_2\text{L}$  (22 mg, 0.10 mmol) was dissolved in 1 mL of formamide. The resulting mixture was sealed in an 8 mL glass vessel and heated at 85  $^\circ\text{C}$  for 48 h. It was subsequently cooled to room temperature ( $0.2\text{ }^\circ\text{C min}^{-1}$ ), affording colorless crystals of **4**. Yield: 72% (based on Zn). Anal. Calcd for  $\text{C}_{11}\text{H}_{12}\text{N}_2\text{O}_7\text{Zn}$  ( $M = 349.60$ ): C, 37.79; H, 3.46; N, 8.01. Found: C, 36.88; H, 3.01; N, 8.10. FT-IR (KBr,  $\text{cm}^{-1}$ ): 3373 (bs), 3177 (bs), 2916 (w), 1698 (s), 1637 (s), 1562 (s), 1444 (s), 1419 (m), 1384 (s), 1329 (s), 1283 (m), 1257 (w), 1112 (m), 1085 (m), 1034 (m), 935 (m), 799 (s), 782 (s), 725 (s), 634 (m), 542 (m), 474 (m).

**Synthesis of 5.** A mixture of  $\text{Zn}(\text{NO}_3)_2 \cdot 6\text{H}_2\text{O}$  (29 mg, 0.10 mmol),  $\text{H}_2\text{L}$  (22 mg, 0.10 mmol), and 4,4'-bipyridine (15.6 mg, 0.10 mmol) was dissolved in 1 mL of DMF and methanol (1:1). A white precipitate was obtained when 0.5 mL of 28% aqueous ammonia solution was added to this reaction mixture. The precipitate was dissolved upon the addition of additional 0.5 mL of 28% aqueous ammonia solution. Then, the resulting mixture was sealed in an 8 mL glass vessel and heated at 75  $^\circ\text{C}$  for 48 h. It was subsequently cooled to room temperature ( $0.2\text{ }^\circ\text{C min}^{-1}$ ), affording plate-like colorless crystals of **5**. Yield: 61% (based on Zn). Anal. Calcd for  $\text{C}_{58}\text{H}_{58}\text{N}_{10}\text{O}_{18}\text{Zn}_3$  ( $M = 1379.28$ ): C, 50.51; H, 4.24; N, 10.16. Found: C, 49.83; H, 4.92; N, 10.09. FT-IR (KBr,  $\text{cm}^{-1}$ ): 3421 (bs), 2962 (w), 1676 (s), 1612 (s), 1571 (s), 1490 (w), 1417 (m), 1385 (s), 1282 (w), 1249 (w), 1217 (w), 1072 (m), 1047 (w), 809 (s), 783 (s), 717 (w), 642 (m), 532 (w).

Scheme 1. Synthesis and Structural Representation (Repeating Units) of 1–3



Scheme 2. Synthesis and Structural Representation (Repeating Units) of 4 and 5



**Crystal Structure Determinations.** X-ray quality single crystals of the compounds were immersed in cryo-oil, mounted in a nylon loop, and measured at room temperature (**1–5**). Intensity data were collected using a Bruker APEX-II PHOTON 100 diffractometer with graphite monochromated Mo-K $\alpha$  ( $\lambda$  0.71069) radiation. Data were collected using phi and omega scans of  $0.5^\circ$  per frame, and a full sphere of data was obtained. Cell parameters were retrieved using Bruker SMART<sup>80–82</sup> software and refined using Bruker SAINT<sup>80</sup> on all the observed reflections. Absorption corrections were applied using SADABS.<sup>80</sup> Structures were solved by direct methods by using the SHELXS-97 package<sup>81</sup> and refined with SHELXL-97.<sup>81</sup> Calculations were performed using the WinGX System, Version 1.80.03.<sup>82</sup> The hydrogen atoms attached to carbon atoms and to the nitrogen atoms were inserted at geometrically calculated positions and included in the refinement using the riding-model approximation;  $U_{\text{iso}}(\text{H})$  was defined as  $1.2U_{\text{eq}}$  of the parent nitrogen atoms or the carbon atoms for phenyl

and methylene residues, and  $1.5U_{\text{eq}}$  of the parent carbon atoms for the methyl groups. The hydrogen atoms of coordinated water molecules were located from the final difference Fourier map, and the isotropic thermal parameters were set at 1.5 times the average thermal parameters of the belonging oxygen atoms. Least square refinements with anisotropic thermal motion parameters for all the non-hydrogen atoms and isotropic ones for the remaining atoms were employed. Crystallographic data are summarized in **Table S1** (Supporting Information), and selected bond distances and angles are presented in **Table S2**. CCDC 1046910–1046914 contain the supplementary crystallographic data for this paper. These data can be obtained free of charge from the Cambridge Crystallographic Data Centre via [www.ccdc.cam.ac.uk/data\\_request/cif](http://www.ccdc.cam.ac.uk/data_request/cif).

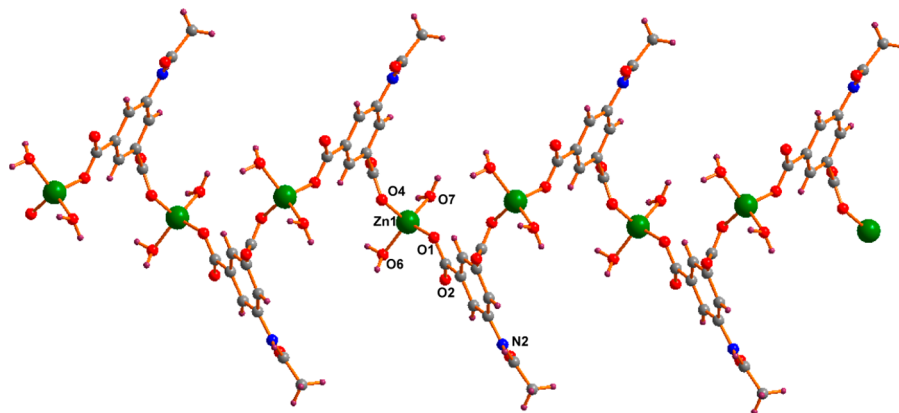


Figure 1. A structural unit of the helical type 1D chain of **1** with partial atom labeling scheme.

## RESULTS AND DISCUSSION

**Syntheses and Characterization.** The hydrothermal reaction, at 75 °C, of 5-acetamidoisophthalic acid ( $H_2L$ ) with zinc(II) nitrate hexahydrate (in stoichiometric amounts) in the presence of dimethylformamide and methanol mixture, formamide or *N*-methylformamide leads to the formation of  $[Zn(L)(H_2O)_2]_n$  (**1**),  $[Zn(L)(H_2O)_2]_n \cdot n(\text{formamide})$  (**2**), or  $[Zn(L)(H_2O)_2]_n \cdot n(N\text{-methylformamide})$  (**3**), respectively ( $L = 5\text{-acetamidoisophthalate}$ ) (Scheme 1). When the hydrothermal reaction of  $H_2L$  with zinc(II) nitrate hexahydrate is performed in a different molar ratio (1:2) and at a higher temperature (85 °C),  $[Zn(L)(H_2O)(\text{formamide})]_n$  (**4**) is formed (Scheme 2). In the presence of 4,4'-bipyridine and in a mixture of DMF and methanol,  $[Zn_3(L)_2(\text{formate})(4,4'\text{-bipyridine})_3]_n \cdot 2n(\text{DMF}) \cdot 2n(H_2O)$  (**5**) is obtained (Scheme 2). During the hydrothermal processes, DMF was hydrolyzed to dimethylamine and formic acid, the latter coordinating the metal in the basic form.

Because of their insolubility in common solvents, the NMR spectra of these frameworks could not be run, but they were characterized by IR spectroscopy, single crystal X-ray diffraction, and thermogravimetric and elemental microanalysis.

In the IR spectra, the characteristic strong bands of coordinated carboxylate groups in **1–5** appear at 1580–1562  $\text{cm}^{-1}$  and 1385–1326  $\text{cm}^{-1}$  for the asymmetric and the symmetric stretching wavenumbers, respectively. The bands in the regions of 1637–1612  $\text{cm}^{-1}$  and 1424–1417  $\text{cm}^{-1}$  are attributed to the C=C stretching frequency of the aromatic rings,<sup>83,84</sup> and those at 1698–1676  $\text{cm}^{-1}$  to the C=O of the amide group.

**Crystal Structure Analysis.** Compounds **1–5** crystallize in space groups  $P2_1$  (**1**),  $P2_1/m$  (**2**),  $P\bar{1}$  (**3** and **4**), and  $C2/c$  (**5**). Compound **1** has a left-handed helix, while **2** and **3** have zigzag type 1D chains; compound **4** features a 1D chain of fused 16- and 8-membered metallacycles and **5** a 2D architecture with 4,4'-bipyridine as secondary ligand.

The structural units of **1**, **2**, and **3** are similar. These polymers are pseudo-polymorphic species owing to the absence (in **1**) or presence of solvent molecules (in **2** and **3**). The asymmetric units of **1–3** contain one zinc(II) ion, one  $L^{2-}$  ligand, two (or only one, in **2**) coordinated water molecules, and one noncoordinated molecule of formamide (in **2**) or *N*-methylformamide (in **3**) (Scheme 1). The asymmetric unit of **4** also contains one  $L^{2-}$  ligand and one the  $Zn^{2+}$  ion and, additionally, one coordinated water and one coordinated formamide molecules, while that of **5** encompasses one  $L^{2-}$

ligand and one formate moiety, two zinc cations, one and a half bipyridine, and a noncoordinated DMF and water molecules.

The  $Zn^{2+}$  ions assume tetrahedral geometries in **1** and **2** ( $\tau_4 = 0.93$  and 0.83, respectively),<sup>85</sup> trigonal bipyramidal in **3** and **4** ( $\tau_5 = 0.54$  and 0.62, respectively),<sup>86</sup> and octahedral in **5** where Zn1 is in a more distorted environment compared to Zn2, as demonstrated by the corresponding quadratic elongations and angle variances (1.073 and  $181.20^{\circ}$  against 1.001 and  $2.32^{\circ}$ , in this order).<sup>87</sup>

The coordination types of the carboxylate groups in **1–5** are diverse, assuming the nonbridging monodentate mode in **1** and **2**. This type of linkage also occurs in **3** and **4** with, additionally, the chelating bidentate fashion in the former and the bridging bidentate (*syn-syn-μ-carboxylate*) in the latter. The bridging bidentate chelation mode (*syn-syn-type*) is the one present in **5**.

The coplanarity of the carboxylate groups and the phenyl ring in  $L^{2-}$  are worth mentioning, being expressed by the  $C_{\text{aromatic}}C_{\text{aromatic}}C_{\text{carboxylate}}O$  (hereafter denoted by CCCO) torsion angles. In **1** this parameter assumes values of  $129.2(4)^{\circ}$  and  $178.7(4)^{\circ}$ , thus giving rise to ZnOCO torsion angles of  $23.3(5)^{\circ}$  and  $11.0(5)^{\circ}$ , in this order, ultimately resulting in the helical nature of this polymer (Figure 2). The CCCO and the ZnOCO torsion angles in **2** are of  $180^{\circ}$  and  $0.0^{\circ}$ , respectively, the reason why this 1D polymer is markedly flat. Polymers **3–5** present CCCO and ZnOCO torsion angles that vary in the ranges of  $166.9(3)$ – $179.1(2)^{\circ}$  and  $3.1(3)$ –

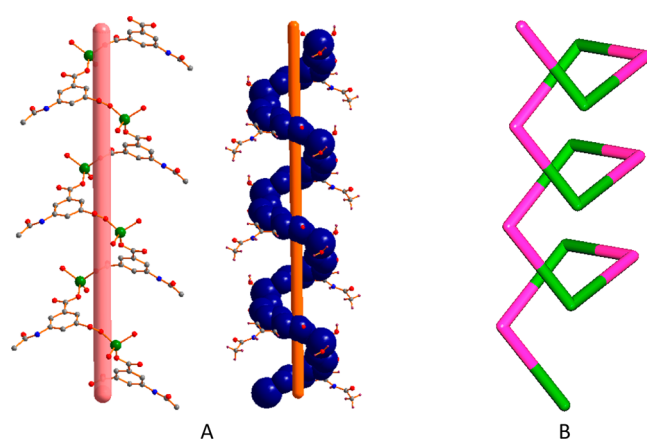
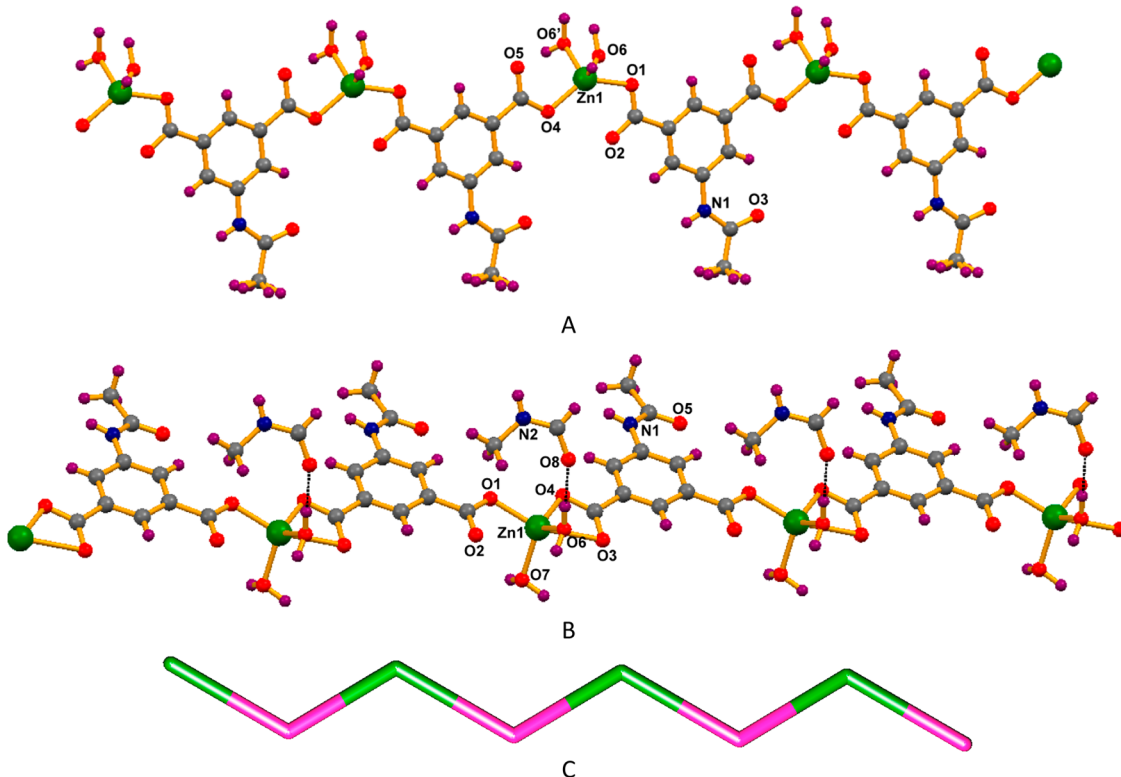


Figure 2. (A) Left-handed helical structure of **1**. (B) Node-and-linker-type descriptions of the 1D coordination framework in **1**, the metal nodes being represented in green and the linkers in pink.



**Figure 3.** Crystal structures of **2** (A) and **3** (B) with partial atom labeling schemes. (C) Node-and-linker-type descriptions of the 1D coordination frameworks in **2** and **3**, the metal nodes being represented in green and the linkers in pink.

18.2(6) $^{\circ}$ , respectively. Concerning the acetamido C<sub>aromatic</sub>NCC torsion angles, they adopt values higher than 171.7(4) $^{\circ}$  evidencing the approximate coplanarity (precise, in the case of **2**) between this group and the phenyl ring.

The Zn–O bond distances are in the usual range of 1.943(2)–2.630(4) Å, the highest value only found in **5** and resulting from the chelating bidentate coordination mode of formate, but still within the sum of the van der Waals radii of Zn and O.

In **4** the metal cations are involved in alternating condensed C<sub>2</sub>O<sub>4</sub>Zn<sub>2</sub> and C<sub>10</sub>O<sub>4</sub>Zn<sub>2</sub> metallacycles that construct a 1D polymeric assembly (Figure 5C).

In **5**, the  $\mu_3$ -L<sub>2</sub><sup>−</sup> and the  $\mu$ -formate ligands bridge the Zn atoms and form  $\sim$ Zn1-( $\mu$ -COO)<sub>L</sub>-( $\mu$ -O)<sub>formate</sub>-Zn2-( $\mu$ -COO)<sub>L</sub>-( $\mu$ -O)<sub>formate</sub>Zn1~ trinuclear cores which are further interconnected giving 16-membered C<sub>10</sub>O<sub>4</sub>Zn<sub>2</sub> rings, thus generating wavelike chain motifs parallel to the ac plane (Figure 6B). These are further extended into a 2D metal–organic layer by means of the  $\mu$ -4,4'-bypiridine. The packing view of **5** is characterized by channels along the crystallographic *a* axis (Figure 6B) with an approximate dimension of 11.39 × 7.59 Å<sup>2</sup>, which are occupied by DMF and water molecules.

The minimum Zn–Zn separation in these polymers vary in the order 3.6878(6) (**4**) < 3.7905(5) (**5**) < 4.3935(5) (**2**) < 4.5627(5) (**3**) < 6.3870(7) (**1**) Å.

Noncovalent interactions (O–H…O, N–H…O and C–H…O; Table S2, Supporting Information) are found in **1–5**, stabilizing the structures and extending them to 3D. The 1D chains of **1** are interconnected via intricate water…carboxylate contacts; the 1D chains of **2** are involved in a 2D network (in the ac plane) by means of NH…O (acetamido…formamide, formamide…acetamido, and formamide…carboxylate) interactions, ultimately expanding to the third dimension by means of

water…carboxylate contacts; the 1D chains of **3** are also tangled in OH…O (water…methylformamide, water…carboxylate, and water…acetamido) and in NH…O (acetamido…methylformamide and methylformamide…carboxylate) contacts.

The noncovalent interactions in **4** (Table S2) are also of the expected types of OH…O (water…acetamido and water…carboxylate) and NH…O (formamide…carboxylate, formamide…acetamido, and acetamido…formamide). The metal–organic network of **5** is reinforced via intermolecular H-bonds (Table S2) involving the crystallization water molecules which simultaneously act as donors (to carboxylate groups) and as acceptors (from the acetamido groups).

Structures **1–3** have similar types of topologies<sup>88,89</sup> and can be represented as 2-connected uninodal nets (Figures 2B and 3C) with topological type 2C1, **4** features a 3-connected uninodal net with a topological type SP1-periodic net (Figure 5D), and **5** reveals a 2,2,2,3,5,6-connected hexanodal net.

**Catalytic Activity of the Zn Coordination Polymers in the Knoevenagel Condensation.** The Knoevenagel condensation (Scheme 3) of aldehydes with active methylene compounds is one of the most useful C–C bond forming reactions having wide applications for the synthesis of fine chemicals.<sup>63–76</sup> This condensation is generally catalyzed by bases or Lewis acids and widely studied in homogeneous systems.<sup>90,91</sup> Only a few studies have employed heterogeneous catalysts including metal organic frameworks.<sup>92–96</sup> Recently, Kitagawa et al.<sup>73</sup> and Zhou et al.<sup>76</sup> reported that amide functionalized MOFs are quite effective for Knoevenagel condensation. Besides that, some Zn-MOFs can also catalyze this condensation in a heterogeneous way.<sup>35,64</sup> Thus, the development of suitable MOFs or coordination polymers based catalysts for this reaction is a topic of great interest.<sup>97,98</sup> It is known that base and acid sites can catalyze this reaction and

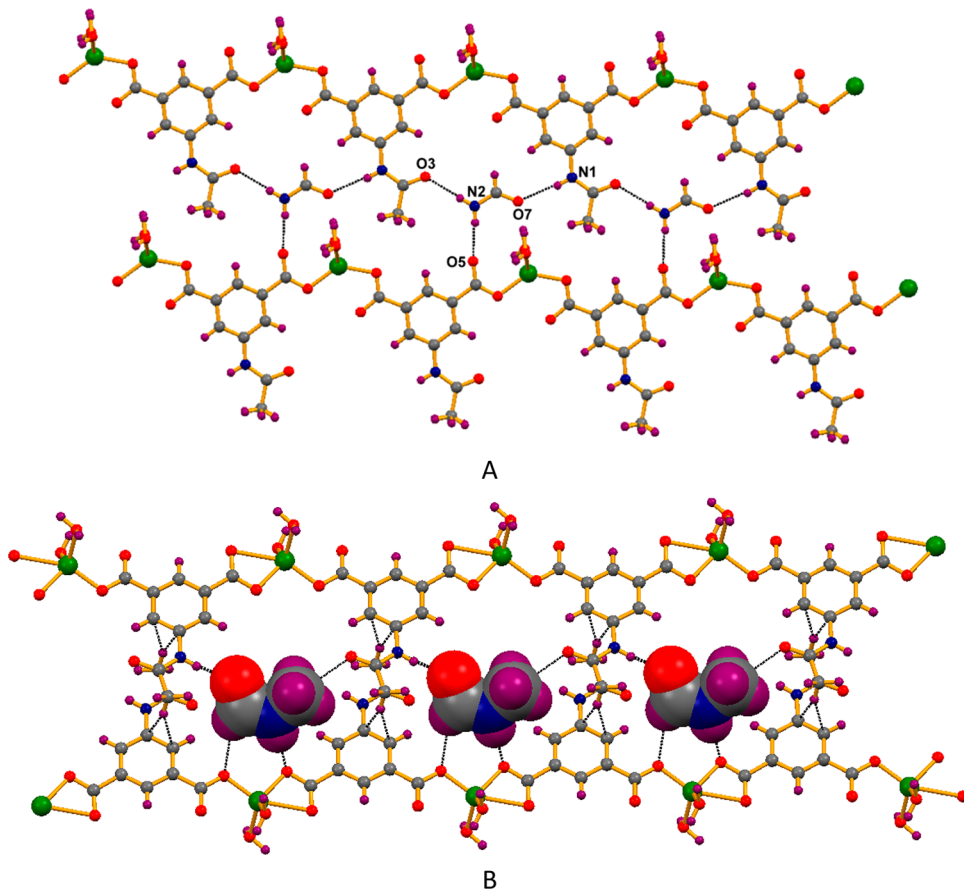


**Figure 4.** Hydrogen bonded networks of **2** (A) and **3** (B) with hydrogen bonding interaction drawn in black dotted lines. *N*-Methylformamide molecules (in B) are represented in the spacefill model.

that bifunctional catalysts (e.g., amide functionalized MOFs) with adequate acid–base pairs are more active than either purely acid or base catalysts.<sup>99–101</sup>

Recently, a few amide functionalized MOFs and Zn-MOFs were separately reported to act as catalysts for the Knoevenagel condensation. Thus, our idea was to produce zinc coordination polymers from an amide functionalized ligand and test their catalytic behavior on this type of reaction. Our newly synthesized zinc(II) coordination polymers have both a Lewis acid ( $Zn^{2+}$ ) and a basic center (amide group), and thus they possibly can act as bifunctional catalysts for this condensation. Moreover, our zinc polymers (**1–5**) have different structural dimensionalities (1D and 2D) and orientations. For example, compounds **1–3** are pseudo-polymorphic supramolecular isomers, having similar 1D type structures but with different structural arrangements and packing. Hence, it would be interesting to see how the different structural features affect the catalytic behavior. To our knowledge only a few examples of supramolecular isomers are known which act as catalysts for the Knoevenagel condensation reactions.<sup>75</sup>

Thus, we have tested the catalytic activity of the coordination polymers **1–5** as solid heterogeneous catalysts in the Knoevenagel condensation of malononitrile with various aldehydes. In a typical reaction, a mixture of benzaldehyde ( $51\ \mu L$ ,  $0.50\ mmol$ ), malononitrile ( $66\ mg$ ,  $1.0\ mmol$ ), and Zn-catalyst ( $5\ mg$  of **1**,  $5.5\ mg$  of **2**,  $6\ mg$  of **3**,  $5\ mg$  of **4**, or  $21\ mg$  of **5**,  $3\ mol\ %$ ) was placed in a capped glass vessel, and then  $1\ mL$  of THF was added into it. The mixture was heated at  $40\ ^\circ C$  for  $1.5\ h$  and subsequently quenched by centrifugation and

filtration at room temperature. The filtrate was evaporated in a vacuum to give the crude product. The residue was dissolved in  $CDCl_3$  and analyzed by  $^1H$  NMR. The  $^1H$  NMR spectra and the calculation of the yield for compound **3** in the Knoevenagel reaction are presented in the Supporting Information (Figure S3).

By using benzaldehyde as a test compound, we found that **3** led to the highest product yield, as compared to the other polymers after the same reaction time and at the same temperature. Consequently, the optimization of the reaction conditions (temperature, reaction time, amount of catalyst, solvent) was carried out in a model malononitrile–benzaldehyde system with **3** as the catalyst (Scheme 2 with typical reaction conditions; Table 1).

Under the above typical conditions ( $3\ mol\ %$  of solid **3** at  $40\ ^\circ C$  with THF as the best solvent, as indicated below), a conversion of  $98\%$  of benzaldehyde into 2-benzylidene malononitrile is reached (entry 5, Table 1) after  $1.5\ h$ . With compounds **1**, **2**, **4**, and **5**, yields of  $91\%$ ,  $89\%$ ,  $78\%$ , and  $61\%$  were obtained, respectively. Hence, our five coordination polymers activities follow the order of  $3 > 1 \approx 2 > 4 > 5$ . The relationship between structure and catalytic activity in the present study is not clearly understood. However, the highest conversion shown by the compound **3** may be due its packing arrangement where the 1D chains are hydrogen bonded with one another and form a 2D sheet. The *N*-methyl formamide molecules trapped inside may eventually assist the substrate molecules (benzaldehyde and malononitrile) to form acid base

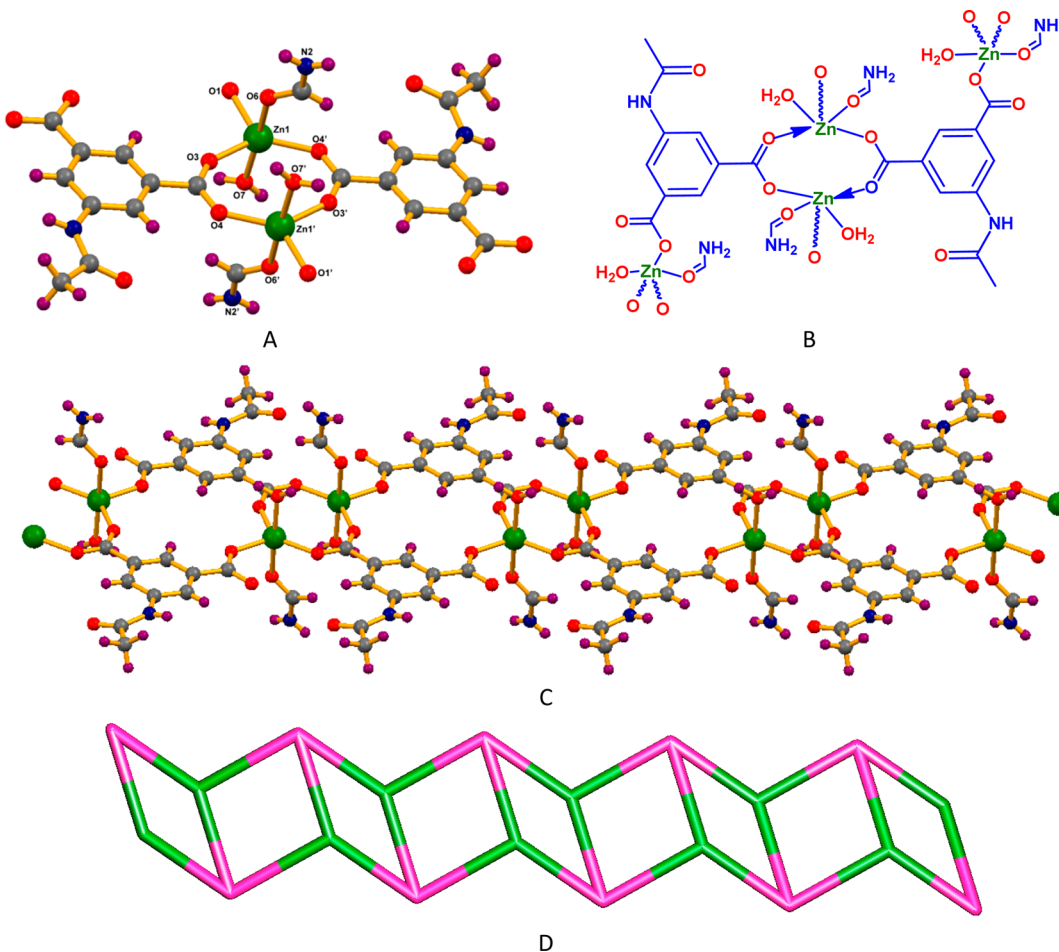


**Figure 5.** Perspective view with partial atom labeling scheme (A) and schematic representation (B) of a fragment of polymer 4. (C) One dimensional structure of complex 4 running along the crystallographic *c* axis. (D) Node-and-linker-type descriptions of 4, the metal nodes being represented in green and the linkers in pink color.

pairs with metal centers. In the other cases (for **1**, **2**, **4**, and **5**), the tight packing does not support the above hypothesis.

The plot of yield versus time for the Knoevenagel condensation reaction of benzaldehyde and malononitrile with compound **3** is presented in Figure 7A.

Blank reactions were tested with benzaldehyde in the absence of catalyst, at 40 °C in THF, and no conversion of aldehyde into 2-benzylidenemalononitrile was detected, after 1.5 h (entry 19, Table 1). The reaction also did not take place by using the free ligand H<sub>2</sub>L instead of catalyst **3** (entry 20, Table 1). We have also checked the reactivity of different zinc(II) salts and ZnO in THF, and the obtained reaction yields are much lower, in the range of 22–43% (entries 21–25, Table 1). Moreover, we have performed this condensation reaction by using 1:1 mixtures of ligand H<sub>2</sub>L and Zn(II) salts, and the obtained yields lie between 21 and 30% (entries 26–28, Table 1), not supporting a catalytic cooperative role. In addition, we have also tested the activity of various metal oxides (different particle size) toward the same reaction under similar conditions, and the observed yields are in the 9–53% range (entries 29–34, Table 1). The obtained results indicate that our catalyst **3** is much better than the tested metal oxides under equivalent reaction conditions.

The effects of temperature, catalyst amount, and solvents were also tested. The increase of the amount of catalyst **3** from 1.0 to 3.0 mol % enhances the product yield from 77 to 98%,

but a further increase in the amount of catalyst leads to no significant increase in catalytic activity (entries 6–8, Table 1).

To select the most suitable solvent, experiments with various solvents (CH<sub>3</sub>CN, CH<sub>2</sub>Cl<sub>2</sub>, THF, and MeOH) have been carried out with compound **3**, and the corresponding plots of yield vs time are presented in Figure 7B. The results indicate that THF (yield of 98%) is the best solvent, whereas the worst one is CH<sub>2</sub>Cl<sub>2</sub> (70% yield) for the same reaction time (1.5 h) (Table 1, entries 5 and 10). In methanol or acetonitrile, a yield of 86% or 75%, respectively, was obtained (Table 1, entries 9 and 11) after 1.5 h. Increasing the temperature from 15 to 40 °C improved the 2-benzylidenemalononitrile yield from 40 to 98% (entries 12 and 5, Table 1). However, we have obtained 97% yield in 6 h at 15 °C (room temperature) (entry 13, Table 1).

We also investigated the catalytic activity of **3** with different types of substituted aromatic aldehydes in the reaction with malononitrile. The results are summarized in Table 2. *p*-Nitrobenzaldehyde produced the maximum yield (100%), while the lowest one (26%) was obtained for *p*-methoxybenzaldehyde, suggesting that an electron-withdrawing substituent promotes the reactivity, in contrast to an electron-donating moiety, what may be related with an increase of the electrophilicity of the substrate in the former case.

In order to perform the catalyst recycling experiments, the used catalyst **3** (separated by centrifugation of the supernatant

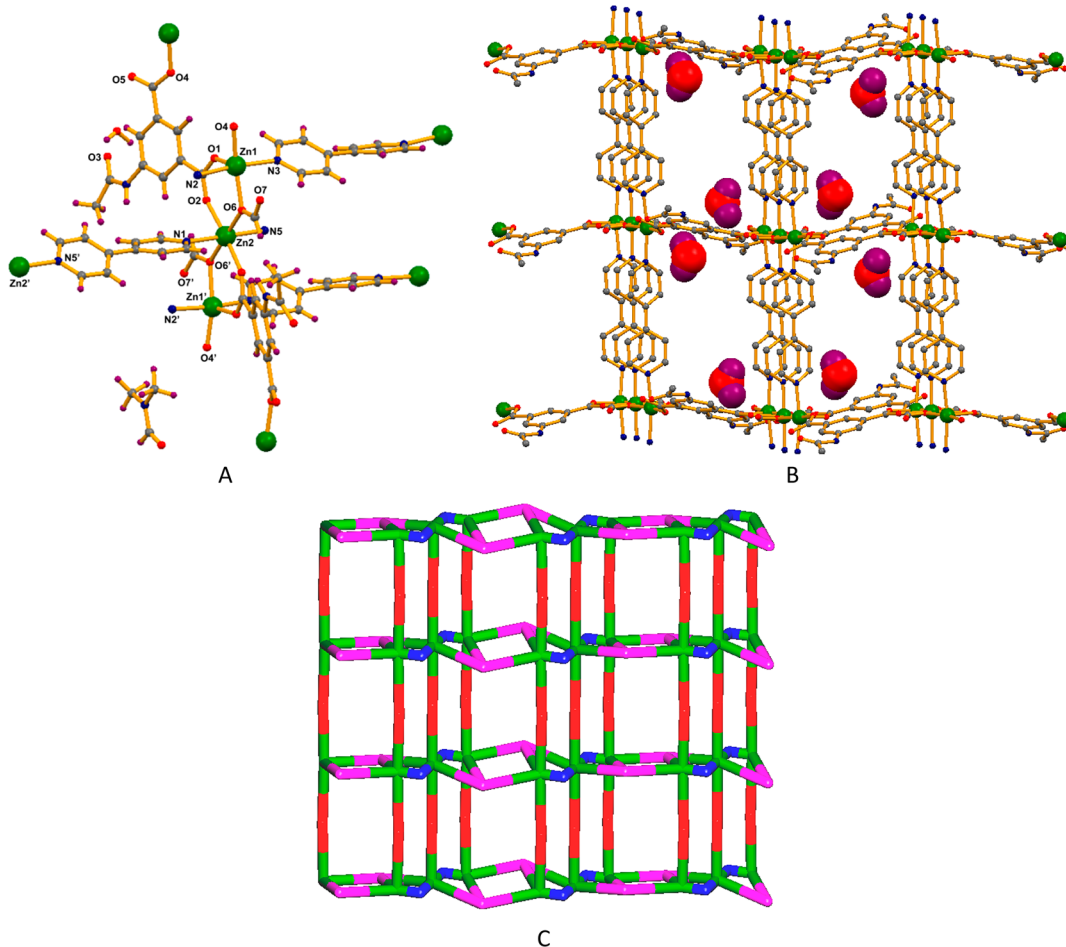
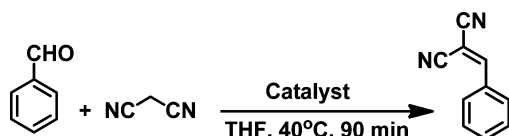


**Figure 6.** (A) Trinuclear secondary building block unit of the coordination polymer 5 with partial atom labeling scheme. (B) 2D packing diagram of 5 (water molecules are represented as spacefill model). (C) Node-and-linker-type descriptions of 5, the metal nodes being represented in green, the linkers in pink, 4,4'-bipyridine in red, and formate anion in blue.

**Scheme 3. Knoevenagel Condensation Reaction of Benzaldehyde with Malononitrile**



solution) was washed with THF and dried in air. It was then reused for the Knoevenagel condensation reaction as described above. The catalyst 3 was recycled in three consecutive experiments, and its activity remained essentially the same (Figure S1). FT-IR spectra of catalyst 3 taken before and after the reaction suggest that the structure of the solid was retained (Figure S2A). We have also performed powder X-ray diffraction with internal standard (NaCl) of catalyst 3 before and after the condensation reaction and observed only a slight difference (2%) in peak intensity after the reaction (Figure S2B). These experiments are indicative that the material essentially remains intact during the catalytic process.

To further verify the heterogeneity of the system, a procedure similar to that of Sheldon et al. was followed.<sup>102</sup> We performed a controlled experiment, removed the catalyst by centrifugation, and the catalyst free reaction solution was kept under the same conditions and monitored by NMR along the time to determine whether the metal component dissolved

appreciably from the solid structure of our catalyst. In our experiment, the catalyst 3 was removed by filtration from the mixture once the conversion was up to ca. 53% (after 30 min reaction time), whereupon the supernatant fluid was stirred for an additional 1 h under the same reaction conditions. As shown in Figure 7A, after separation of the solid catalyst, no conversion of benzaldehyde is observed. These results demonstrate that the catalysis is heterogeneous in nature. Additionally, the filtrate solution, after the separation of the catalyst, was evaporated to dryness and the amount of zinc was determined, being only 0.02% of the amount used in the reaction, thus ruling out any significant leaching of the catalyst.

There are some reports on coordination polymers which are catalysts for this kind of reaction,<sup>63–76</sup> and a comparison with our catalyst 3 is shown in Table 3. The obtained yields in our system are usually higher than for the other reported zinc(II) frameworks in which the reaction of benzaldehyde and malononitrile, after a longer time and at a higher temperature, leads to an overall yield that is lower or identical to ours (Table 3, entries 2 and 3).<sup>69,70</sup> Similarly, a 3D metal–organic framework built from nickel(II) ions as connectors and methanetetrabenoate ligands produced 78% yield after 6 h at 130 °C (Table 2, entry 4).<sup>71</sup> Moreover, when we performed the reaction at room temperature with our catalyst 3, a 97% yield was reached only in 6 h (Table 3, entry 6), which is a much lower time than those for other reported Cd(II) and Pb(II)-

**Table 1.** Optimization of the Parameters of the Knoevenagel Condensation Reaction between Benzaldehyde and Malononitrile with 3 as the Catalyst<sup>a</sup>

entry	catalyst	time (h)	amount of catalyst (mol %)	T (°C)	solvent	yield (%) <sup>b</sup>	TON <sup>c</sup>
1	3	0.25	3.0	40	THF	33	11
2	3	0.5	3.0	40	THF	53	18
3	3	0.75	3.0	40	THF	63	21
4	3	1	3.0	40	THF	76	25
5	3	1.5	3.0	40	THF	98	33
6	3	1.5	1.0	40	THF	77	77
7	3	1.5	5.0	40	THF	97	18
8	3	1.5	7.0	40	THF	98	14
9	3	1.5	3.0	40	CH <sub>3</sub> CN	86	29
10	3	1.5	3.0	40	CH <sub>2</sub> Cl <sub>2</sub>	70	23
11	3	1.5	3.0	40	MeOH	75	25
12	3	1.5	3.0	RT (15 °C)	THF	40	13
13	3	6.0	3.0	RT (15 °C)	THF	97	32
14	3	1.5	3.0	25	THF	88	29
15	1	1.5	3.0	40	THF	91	30
16	2	1.5	3.0	40	THF	89	29
17	4	1.5	3.0	40	THF	78	26
18	5	1.5	3.0	40	THF	61	20
19	blank	1.5		40	THF	no reaction	
20	H <sub>2</sub> L	1.5	3.0	40	THF	no reaction	
21	Zn(NO <sub>3</sub> ) <sub>2</sub> ·6H <sub>2</sub> O	1.5	3.0	40	THF	41	14
22	Zn(OAc) <sub>2</sub> ·2H <sub>2</sub> O	1.5	3.0	40	THF	39	13
23	ZnSO <sub>4</sub> ·7H <sub>2</sub> O	1.5	3.0	40	THF	22	7
24	ZnCl <sub>2</sub>	1.5	3.0	40	THF	29	10
25	ZnO	1.5	3.0	40	THF	43	14
26	H <sub>2</sub> L + Zn(NO <sub>3</sub> ) <sub>2</sub> ·6H <sub>2</sub> O	1.5	3.0	40	THF	24	8
27	H <sub>2</sub> L + ZnSO <sub>4</sub> ·7H <sub>2</sub> O	1.5	3.0	40	THF	21	7
28	H <sub>2</sub> L + ZnCl <sub>2</sub>	1.5	3.0	40	THF	30	10
29	Al <sub>2</sub> O <sub>3</sub>	1.5	3.0	40	THF	21	7
30	V <sub>2</sub> O <sub>5</sub>	1.5	3.0	40	THF	25	8
31	CdO	1.5	3.0	40	THF	53	17
32	MoO <sub>3</sub>	1.5	3.0	40	THF	13	4
33	PbO <sub>2</sub>	1.5	3.0	40	THF	9	3
34	HgO	1.5	3.0	40	THF	26	8

<sup>a</sup>Reaction conditions: 3.0 mol % of catalyst 3, solvent (THF) 1 mL, malononitrile (66 mg, 1.0 mmol), and benzaldehyde (0.50 mmol). <sup>b</sup>Calculated by <sup>1</sup>H NMR. <sup>c</sup>Number of moles of product per mole of catalyst.

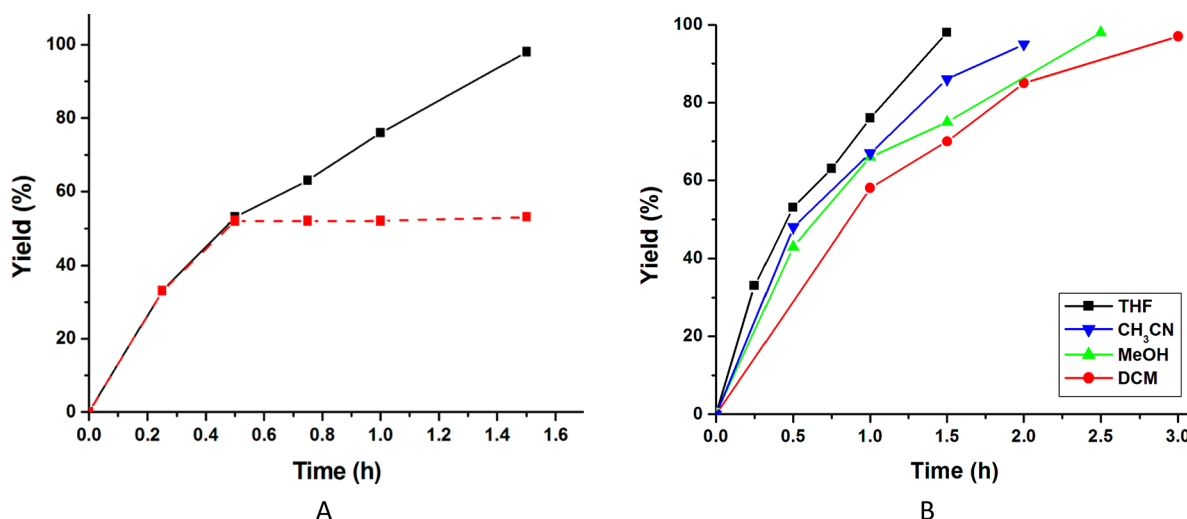


**Figure 7.** Plots of yield vs time for the Knoevenagel condensation reaction of benzaldehyde and malononitrile in the presence of catalyst 3. (A) In THF (black curve) and upon separation of catalyst 3 (red curve). (B) In the presence of several solvents.

Table 2. Knoevenagel Condensation Reaction of Various Aldehydes with Malononitrile with Catalyst 3<sup>a</sup>

Entry	compound	Yield <sup>b</sup> (%)	TON <sup>c</sup>
1	O <sub>2</sub> N-C <sub>6</sub> H <sub>4</sub> -CHO	100	33
2	H <sub>3</sub> CO-C <sub>6</sub> H <sub>4</sub> -CHO	26	8
3	Cl-C <sub>6</sub> H <sub>4</sub> -CHO	94	31
4	H <sub>3</sub> C-C <sub>6</sub> H <sub>4</sub> -CHO	70	23
5	HO-C <sub>6</sub> H <sub>4</sub> -CHO	86	28
6	C <sub>6</sub> H <sub>5</sub> -CH=CHO	69	23

<sup>a</sup>Reaction conditions: 3.0 mol % of catalyst 3, solvent (THF) 1 mL, malononitrile (66 mg, 1.0 mmol), and aldehyde (0.50 mmol); reaction time of 1.5 h. <sup>b</sup>Calculated by <sup>1</sup>H NMR. <sup>c</sup>Number of moles of product per mole of catalyst.

Table 3. Comparison of Catalytic Activity of Various Coordination Polymers in the Knoevenagel Condensation Reaction of Benzaldehydes and Malononitrile<sup>a</sup>

entry	catalyst	solvent/temp/time	aldehydes	yield (%)	ref
1	3	THF/40 °C/1.5 h	benzaldehyde	98	this work
2	Zn <sub>2</sub> dobdc	toluene/70 °C/24 h	benzaldehyde	77	69
3	Zn <sub>2</sub> (tpt) <sub>2</sub> (2-atp)I <sub>2</sub>	ethanol/60 °C/2 h	benzaldehyde	99	70
4	{[Ni <sub>4</sub> (μ <sub>6</sub> -MTB) <sub>2</sub> (μ <sub>2</sub> -H <sub>2</sub> O) <sub>4</sub> (H <sub>2</sub> O) <sub>4</sub> ]·10DMF·11H <sub>2</sub> O} <sub>n</sub>	p-xylene/130 °C/6 h	benzaldehyde	78	71
5	[Tb(BTATB) (DMF)-2(H <sub>2</sub> O)]·DMF·2H <sub>2</sub> O	CH <sub>3</sub> CN/60 °C/24 h	benzaldehyde	99	72
6	3	THF/RT/6 h	benzaldehyde	97	this work
7	[Cd(4-btapa) <sub>2</sub> (NO <sub>3</sub> ) <sub>2</sub> ]·6H <sub>2</sub> O·2DMF	C <sub>6</sub> H <sub>6</sub> /RT/12 h	benzaldehyde	98	73
8	Pb(cpna) <sub>2</sub> ·2DMF·6H <sub>2</sub> O	CH <sub>3</sub> CN/RT/24 h	benzaldehyde	100	74
9	3	THF/40 °C/1.5 h	4-nitrobenzaldehyde	100	this work
10	{[Cd(NH <sub>2</sub> -bdc) (bphz) <sub>0.5</sub> ]·DMF·H <sub>2</sub> O} <sub>n</sub>	CH <sub>3</sub> CN/60 °C/6 h	4-nitrobenzaldehyde	99	75

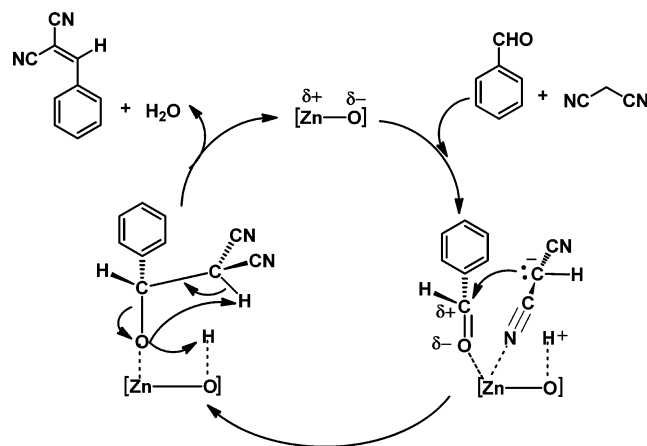
<sup>a</sup>dobdc = 2,5-dioxidoterephthalate; MTB = methanetetrabenoate; DMF = N,N'-dimethylformamide; BTATB = 4,4',4''-(benzene-1,3,5-triyltris(azanediyl))tribenzoate; 4-btapa = 1,3,5-benzene tricarboxylic acid tris[N-(4-pyridyl)amide]; cpna = N-(4-carboxyphenyl)isonicotinamide 1-oxide; NH<sub>2</sub>-bdc = 2-aminobenzenedicarboxylic acid; bphz = 1,2-bis(4-pyridylmethylene) hydrazine; tpt = tris (4-pyridyl) triazine; 2-atp = 2-aminoterephthalate.

MOFs (Table 3, entries 7 and 8).<sup>73,74</sup> In comparison with other catalysts, ours have the advantages of being rather cheap, easy-to-prepare, and highly active at low temperature. Moreover, they are recyclable without appreciable loss of activity.

A possible mechanism for the Knoevenagel condensation catalyzed by 1–5 is presented in Scheme 4, on the basis of reported proposals.<sup>103</sup> In our coordination polymers, the zinc center (Lewis acid site) interacts with the carbonyl group of the benzaldehyde, producing a polarization of this group and thus

increasing the electrophilic character of the carbonylic carbon atom. This polarization favors the attack from the malononitrile. The interaction of a cyano group of malononitrile with the Lewis acid (zinc site) increases the acidity of the methylene group which enhances the deprotonation of malononitrile. The basic sites (carboxylate-O or amide-O) can abstract the proton from the methylenic group to generate the corresponding nucleophilic species which attacks the carbonyl group of benzaldehyde with C–C bond formation (aldol condensation) and dehydration. If the acid and basic sites of the bifunctional catalysts are well balanced, a concerted and synergic action can take place.

Scheme 4. Proposed Catalytic Cycle for the Knoevenagel Condensation Reaction Catalyzed by 1–5



## CONCLUSION

Five zinc(II) coordination polymers constructed with 5-acetamidoisophthalic acid (H<sub>2</sub>L) were synthesized. They exhibit 1D (**1**, **2**, **3**, and **4**) and 2D (**5**) structures, on account of the various coordination modes of the ligand. Single-crystal X-ray diffraction analysis revealed that **1**, **2**, and **3** are pseudo-polymorphic supramolecular isomers, with **1** having an helical assembly, but **2** and **3** exhibiting similar zigzag type structures containing different guest molecules (formamide in **2** and methylformamide in **3**). Compound **4** is a 1D coordination polymer with fused 8-membered and 16-membered dimetallic rings, whereas compound **5** shows a two-dimensional layered structure with trimetallic cores. Zinc(II) coordination numbers and geometries vary from tetrahedral (in **1** and **2**) to trigonal bipyramidal (in **3** and **4**) and to octahedral (in **5**).

These coordination polymers act as heterogeneous catalysts for the Knoevenagel condensation of aldehydes with malononitrile, at moderate temperature. Among the five coordination polymers, 3 is the most effective catalyst for this condensation reaction. It effectively catalyzes the reaction of various aldehydes and malononitrile producing the corresponding benzylidenemalononitriles in high yields, which depend on the electrophilicity of the substrate. Moreover, the catalyst is stable and recyclable. Moreover, the present study displays an example of pseudo-polymorphic supramolecular isomers acting as heterogeneous catalysts for the Knoevenagel condensation. It also presents the dependence of the catalytic properties on the supramolecular structural arrangements.

This study also provides further evidence that zinc(II) coordination polymers can be utilized as effective heterogeneous catalysts, under mild conditions, in this important organic reaction. Further explorations into the uses of this catalyst family in other organic transformations, as well as mechanistic investigations, are ongoing.

## ■ ASSOCIATED CONTENT

### Supporting Information

The Supporting Information is available free of charge on the ACS Publications website at DOI: [10.1021/acs.cgd.5b00948](https://doi.org/10.1021/acs.cgd.5b00948).

Bond distances, angles, and hydrogen bonding tables for all compounds (1–5), thermogravimetric analysis, FT-IR, and PXRD before and after catalysis, <sup>1</sup>H NMR spectra after catalysis, curve for recycling experiment

(PDF)

CIF files and crystallographic data (CIF)

## ■ AUTHOR INFORMATION

### Corresponding Authors

\*(A.K.) E-mail: [anirbanchem@gmail.com](mailto:anirbanchem@gmail.com).

\*(M.F.C.G.S.) E-mail: [fatima.guedes@tecnico.ulisboa.pt](mailto:fatima.guedes@tecnico.ulisboa.pt).

\*(A.J.L.P.) E-mail: [pombeiro@tecnico.ulisboa.pt](mailto:pombeiro@tecnico.ulisboa.pt).

### Notes

The authors declare no competing financial interest.

## ■ ACKNOWLEDGMENTS

This work has been supported by the Foundation for Science and Technology (FCT), Portugal (Project UID/QUI/00100/2013). A.K. and S.H. express their gratitude to the FCT for postdoctoral fellowships (Ref. No. SFRH/BPD/76192/2011 and SFRH/BPD/78264/2011). Authors M.F.C.G.S. and A.J.L.P. also acknowledge the Russian Science Foundation for support to the synthesis with malononitrile and for the help in organizing the International Laboratory (Grant 14-43-00017). Thanks are also due to the Portuguese NMR Network (IST-UL Centre) for access to the NMR facility and the IST Node of the Portuguese Network of mass-spectrometry (Dr. Conceição Oliveira) for the ESI-MS measurements.

## ■ REFERENCES

- (1) Batten, S. R.; Champness, N. R.; Chen, X.-M.; Garcia-Martinez, J.; Kitagawa, S.; Öhrström, L.; O'Keeffe, M.; Suh, M. P.; Reedijk, J. *Pure Appl. Chem.* **2013**, *85*, 1715–1724.
- (2) Zhou, H. -C. J.; Kitagawa, S. *Chem. Soc. Rev.* **2014**, *43*, 5415–5418.
- (3) Lin, Z.-J.; Lü, J.; Hong, M.; Cao, R. *Chem. Soc. Rev.* **2014**, *43*, 5867–5895.
- (4) Karmakar, A.; Goldberg, I. *CrystEngComm* **2011**, *13*, 350–366.
- (5) Karmakar, A.; Goldberg, I. *CrystEngComm* **2011**, *13*, 339–349.
- (6) O'Keeffe, M.; Yaghi, O. M. *Chem. Rev.* **2012**, *112*, 675–702.
- (7) He, Y.; Zhou, W.; Qian, G.; Chen, B. *Chem. Soc. Rev.* **2014**, *43*, 5657–5678.
- (8) Suh, M. P.; Park, H. J.; Prasad, T. K.; Lim, D.-W. *Chem. Rev.* **2012**, *112*, 782–835.
- (9) *Metal-Organic Frameworks: Design and Application*; MacGillivray, L. R., Ed.; Wiley-VCH: Weinheim, Germany, 2010.
- (10) *Metal-Organic Framework Materials*; MacGillivray, L. R., Lukehart, C. M., Eds.; Wiley-VCH: Weinheim, Germany, 2014.
- (11) *Functional Metal-Organic Frameworks: Gas Storage, Separation and Catalysis*; Schröder, M., Ed.; Topics in Current Chemistry, Springer-Verlag: Berlin, 2010.
- (12) Rowsell, J. L. C.; Yaghi, O. M. *Angew. Chem., Int. Ed.* **2005**, *44*, 4670.
- (13) Rosi, N. L.; Eckert, J.; Eddaoudi, M.; Vodak, D. T.; Kim, J.; O'Keeffe, M.; Yaghi, O. M. *Science* **2003**, *300*, 1127–1129.
- (14) Kesani, B.; Cui, Y.; Smith, M. R.; Bittner, E. W.; Bockrath, B. C.; Lin, W. *Angew. Chem., Int. Ed.* **2005**, *44*, 72–75.
- (15) Kitagawa, S.; Kitaura, R.; Noro, S. *Angew. Chem., Int. Ed.* **2004**, *43*, 2334–2375.
- (16) Kitaura, R.; Seki, K.; Akiyama, G.; Kitagawa, S. *Angew. Chem., Int. Ed.* **2003**, *42*, 428.
- (17) Horcajada, P.; Serre, C.; Maurin, G.; Ramsahye, N. A.; Balas, F.; Vallet-Regí, M.; Sebban, M.; Taulelle, F.; Férey, G. *J. Am. Chem. Soc.* **2008**, *130*, 6774.
- (18) Horcajada, P.; Serre, C.; Vallet-Regí, M.; Sebban, M.; Taulelle, F.; Férey, G. *Angew. Chem., Int. Ed.* **2006**, *45*, 5974.
- (19) Meilikov, M.; Yusenko, K.; Esken, D.; Turner, S.; Van Tendeloo, G.; Fischer, R. A. *Eur. J. Inorg. Chem.* **2010**, *2010*, 3701–3714.
- (20) Fromm, K. M.; Sagué, J. L.; Mirolo, L. *Macromol. Symp.* **2010**, *291*–292, 75–83.
- (21) Zhang, J. – P.; Huang, X. – C.; Chen, X. – M. *Chem. Soc. Rev.* **2009**, *38*, 2385–2396.
- (22) Batten, S. R.; Neville, S. M.; Turner, D. R. *Malleability of Coordination Polymers*, *Coordination Polymers: Design, Analysis and Application*; The Royal Society of Chemistry: Cambridge, UK, 2009; pp 96–143.
- (23) Schröder, M.; Champness, N. R. *Encyclopedia of Supramolecular Chemistry*; Atwood, J. L., Steed, J. W., Eds.; CRC Press: Boca Raton, FL, 2004; Vol. 2, pp 1420–1426.
- (24) Moulton, B.; Zaworotko, M. J. *Chem. Rev.* **2001**, *101*, 1629.
- (25) Hennigar, T. L.; MacQuarrie, D. C.; Losier, P.; Rogers, R. D.; Zaworotko, M. J. *Angew. Chem., Int. Ed. Engl.* **1997**, *36*, 972.
- (26) Soldatov, D. J.; Ripmeester, J. A.; Shergina, S. I.; Sokolov, I. E.; Zanina, A. S.; Gromilov, S. A.; Dyadin, Y. A. *J. Am. Chem. Soc.* **1999**, *121*, 4179.
- (27) Lee, I. S.; Shin, D. M.; Chung, Y. K. *Chem. - Eur. J.* **2004**, *10*, 3158–3165.
- (28) Sun, D.; Ke, Y.; Mattox, T. M.; Ooro, B. A.; Zhou, H.-C. *Chem. Commun.* **2005**, 5447–5449.
- (29) Wang, S.-N.; Bai, J.; Li, Y.-Z.; Scheer, M.; You, X.-Z. *CrystEngComm* **2007**, *9*, 228–235.
- (30) Huang, X.-C.; Zhang, J.-P.; Chen, X.-M. *Cryst. Growth Des.* **2006**, *6*, 1194–1198.
- (31) Lee, J.-Y.; Chen, C.-Y.; Lee, H. M.; Passaglia, E.; Vizza, F.; Oberhauser, W. *Cryst. Growth Des.* **2011**, *11*, 1230–1237.
- (32) Ghosh, S.; Mukherjee, S.; Seth, P.; Mukherjee, P. S.; Ghosh, A. *Dalton Trans.* **2013**, *42*, 13554–13564.
- (33) Lee, J. Y.; Farha, O. K.; Roberts, J.; Scheidt, K. A.; Nguyen, S. T.; Hupp, J. T. *Chem. Soc. Rev.* **2009**, *38*, 1450–1459.
- (34) Corma, A.; García, H.; Llabrés i Xamena, F. X. *Chem. Rev.* **2010**, *110*, 4606–4655.
- (35) Dhakshinamoorthy, A.; Opanasenko, M.; Čejka, J.; García, H. *Adv. Synth. Catal.* **2013**, *355*, 247–268.
- (36) Karmakar, A.; Hazra, S.; Guedes da Silva, M. F. C.; Pombeiro, A. J. L. *Dalton Trans.* **2015**, *44*, 268–280.

- (37) Liu, J.; Chen, L.; Cui, H.; Zhang, J.; Zhang, L.; Su, C.-Y. *Chem. Soc. Rev.* **2014**, *43*, 6011–6061.
- (38) Zhang, Y.; Riduan, S. N. *Chem. Soc. Rev.* **2012**, *41*, 2083–2094.
- (39) Valvckens, P.; Vermoortele, F.; De Vos, D. *Catal. Sci. Technol.* **2013**, *3*, 1435–1445.
- (40) Kirillov, A. M.; Kirillova, M. V.; Pombeiro, A. J. L. *Coord. Chem. Rev.* **2012**, *256*, 2741–2759.
- (41) Kirillov, A. M.; Coelho, J. A. S.; Kirillova, M. V.; da Silva, M. F. C. G.; Nesterov, D. S.; Gruenwald, K. R.; Haukka, M.; Pombeiro, A. J. L. *Inorg. Chem.* **2010**, *49*, 6390–6392.
- (42) Karmakar, A.; Titi, H. M.; Goldberg, I. *Cryst. Growth Des.* **2011**, *11*, 2621–2636.
- (43) Dhakshinamoorthy, A.; Alvaro, M.; Corma, A.; Garcia, H. *Dalton Trans.* **2011**, *40*, 6344–6360.
- (44) Zhao, M.; Ou, S.; Wu, C.-D. *Acc. Chem. Res.* **2014**, *47*, 1199–1207.
- (45) Horcajada, P.; Surblé, S.; Serre, C.; Hong, D. Y.; Seo, Y. K.; Chang, J. S.; Grenèche, J. M.; Margiolaki, I.; Férey, G. *Chem. Commun.* **2007**, 2820–2822.
- (46) Jeong, K. S.; Go, Y. B.; Shin, S. M.; Lee, S. J.; Kim, J.; Yaghi, O. M.; Jeong, N. *Chem. Sci.* **2011**, *2*, 877–882.
- (47) Nayak, S.; Harms, K.; Dehnen, S. *Inorg. Chem.* **2011**, *50*, 2714–2716.
- (48) Alaerts, L.; Séguin, E.; Poelman, H.; Thibault-Starzyk, F.; Jacobs, P. A.; De Vos, D. E. *Chem. - Eur. J.* **2006**, *12*, 7353–7363.
- (49) Horike, S.; Dincă, M.; Tamaki, K.; Long, J. R. *J. Am. Chem. Soc.* **2008**, *130*, 5854–5855.
- (50) Jlassi, R.; Ribeiro, A. P. C.; Guedes da Silva, M. F. C.; Mahmudov, K. T.; Kopylovich, M. N.; Anisimova, T. B.; Naili, H.; Tiago, G. A. O.; Pombeiro, A. J. L. *Eur. J. Inorg. Chem.* **2014**, *2014*, 4541–4550.
- (51) Nasani, R.; Saha, M.; Mobin, S. M.; Martins, L. M. D. R. S.; Pombeiro, A. J. L.; Kirillov, A. M.; Mukhopadhyay, S. *Dalton Trans.* **2014**, *43*, 9944–9954.
- (52) Karabach, Y. Y.; Guedes da Silva, M. F. C.; Kopylovich, M. N.; Gil-Hernández, B.; Sanchiz, J.; Kirillov, A. M.; Pombeiro, A. J. L. *Inorg. Chem.* **2010**, *49*, 11096–11105.
- (53) Kirillova, M. V.; Kirillov, A. M.; Guedes da Silva, M. F. C.; Pombeiro, A. J. L. *Eur. J. Inorg. Chem.* **2008**, *2008*, 3423–3427.
- (54) Kirillov, A. M.; Kirillova, M. V.; Pombeiro, A. J. L. In *Advances in Organometallic Chemistry and Catalysis (The Silver/Gold Jubilee ICOMC Celebratory Book)*; Pombeiro, A. J. L., Ed.; J. Wiley & Sons: New York, 2014; Vol. 3, pp 27–38.
- (55) Kirillov, A. M.; Kopylovich, M. N.; Kirillova, M. V.; Yu, E.; Karabach, Y. Y.; Haukka, M.; da Silva, M. F. C. G.; Pombeiro, A. J. L. *Adv. Synth. Catal.* **2006**, *348*, 159–174.
- (56) Leus, K.; Liu, Y. – Y.; Van Der Voort, P. *Catal. Rev.: Sci. Eng.* **2014**, *56*, 1–56.
- (57) Seo, J. S.; Whang, D.; Lee, H.; Jun, S. I.; Oh, J.; Jeon, Y. J.; Kim, K. *Nature* **2000**, *404*, 982–986.
- (58) Dybtsev, D. N.; Nuzhdin, A. L.; Chun, H.; Bryliakov, K. P.; Talsi, E. P.; Fedin, V. P.; Kim, K. *Angew. Chem., Int. Ed.* **2006**, *45*, 916–920.
- (59) Kirillov, A. M.; Karabach, Y. Y.; Kirillova, M. V.; Haukka, M.; Pombeiro, A. J. L. *Dalton Trans.* **2011**, *40*, 6378–6381.
- (60) Contaldi, S.; Di Nicola, C.; Garau, F.; Karabach, Y. Y.; Martins, L. M. D. R. S.; Monari, M.; Pandolfo, L.; Pettinari, C.; Pombeiro, A. J. L. *Dalton Trans.* **2009**, 4928–4941.
- (61) Di Nicola, C.; Karabach, Y. Y.; Kirillov, A. M.; Monari, M.; Pandolfo, L.; Pettinari, C.; Pombeiro, A. J. L. *Inorg. Chem.* **2007**, *46*, 221–230.
- (62) Opanasenko, M.; Shamzhy, M.; Čejka, J. *ChemCatChem* **2013**, *5*, 1024–1031.
- (63) Hartmann, M.; Fischer, M. *Microporous Mesoporous Mater.* **2012**, *164*, 38–43.
- (64) Xamena, F.; Cirujano, F. G.; Corma, A. *Microporous Mesoporous Mater.* **2012**, *157*, 112–117.
- (65) Nguyen, L. T. L.; Le, K. K. A.; Truong, H. X.; Phan, N. T. S. *Catal. Sci. Technol.* **2012**, *2*, 521–528.
- (66) Burgoyne, A. R.; Meijboom, R. *Catal. Lett.* **2013**, *143*, 563–571.
- (67) Fang, Q. – R.; Yuan, D. – Q.; Sculley, J.; Li, J. – R.; Han, Z. – B.; Zhou, H. – C. *Inorg. Chem.* **2010**, *49*, 11637–11642.
- (68) Sharma, M. K.; Singh, P. P.; Bharadwaj, P. K. *J. Mol. Catal. A: Chem.* **2011**, *342*–343, 6–10.
- (69) Valvckens, P.; Vandichel, M.; Waroquier, M.; Van Speybroeck, V.; De Vos, D. *J. Catal.* **2014**, *317*, 1–10.
- (70) Tan, Y.; Fu, Z.; Zhang, J. *Inorg. Chem. Commun.* **2011**, *14*, 1966–1970.
- (71) Almáši, M.; Zeleňák, V.; Opanasenko, M.; Čejka, J. *Dalton Trans.* **2014**, *43*, 3730–3738.
- (72) Wei, N.; Zhang, M. Y.; Zhang, X. N.; Li, G. M.; Zhang, X. D.; Han, Z. B. *Cryst. Growth Des.* **2014**, *14*, 3002–3009.
- (73) Hasegawa, S.; Horike, S.; Matsuda, R.; Furukawa, S.; Mochizuki, K.; Kinoshita, Y.; Kitagawa, S. *J. Am. Chem. Soc.* **2007**, *129*, 2607–2614.
- (74) Lin, X. M.; Li, T. T.; Chen, L. F.; Zhang, L.; Su, C.-Y. *Dalton Trans.* **2012**, *41*, 10422–10429.
- (75) Haldar, R.; Reddy, S. K.; Suresh, V. M.; Mohapatra, S.; Balasubramanian, S.; Maji, T. K. *Chem. - Eur. J.* **2014**, *20*, 4347–4356.
- (76) Park, J.; Li, J. R.; Chen, Y. P.; Yu, J.; Yakovenko, A. A.; Wang, Z. U.; Sun, L.-B.; Balbuena, P. B.; Zhou, H. C. *Chem. Commun.* **2012**, *48*, 9995.
- (77) Opanasenko, M.; Dhakshinamoorthy, A.; Chang, J. S.; Garcia, H.; Čejka, J.; Hwang, Y. K. *ChemSusChem* **2013**, *6*, 865–871.
- (78) Karmakar, A.; Guedes da Silva, M. F. C.; Pombeiro, A. J. L. *Dalton Trans.* **2014**, *43*, 7795–7810.
- (79) Karmakar, A.; Hazra, S.; Guedes da Silva, M. F. C.; Pombeiro, A. J. L. *New J. Chem.* **2014**, *38*, 4837–4846.
- (80) APEX2 & SAINT; Bruker AXS Inc.: Madison, WI, 2004.
- (81) Sheldrick, G. M. *Acta Crystallogr., Sect. A: Found. Crystallogr.* **2008**, *64*, 112–122.
- (82) Farrugia, L. J. *J. Appl. Crystallogr.* **1999**, *32*, 837–838. (d) Spek, A. L. *Acta Crystallogr., Sect. A* **1990**, *46* (Suppl.), C34.
- (83) Nakamoto, K. *Infrared and Raman Spectra of Inorganic and Coordination Compounds*, 5th ed.; Wiley & Sons: New York, 1997.
- (84) Socrates, G. *Infrared Characteristic Group Frequencies*; Wiley: New York, 1980.
- (85) Yang, L.; Powell, D. R.; Houser, R. P. *Dalton Trans.* **2007**, 955–964.
- (86) Munoz-Hernandez, M.-A.; Keizer, T. S.; Wei, P.; Parkin, S.; Atwood, D. A. *Inorg. Chem.* **2001**, *40*, 6782–6787.
- (87) Robinson, K.; Gibbs, G. V.; Ribbe, P. H. *Science* **1971**, *172*, 567–570.
- (88) Blatov, V. A. *IUCr, Comput. Comm. Newslett.* **2006**, *7*, 4 <http://www.topos.ssu.samara.ru/>.
- (89) Blatov, V. A. *Struct. Chem.* **2012**, *23*, 955–963.
- (90) Knoevenagel, E. *Ber. Dtsch. Chem. Ges.* **1898**, *31*, 2585–2595.
- (91) Jones, G. *Org. React.* **1967**, *15*, 204–599.
- (92) Kantam, M. L.; Choudary, B. M.; Reddy, C. V.; Rao, K. K.; Figueras, F. *Chem. Commun.* **1998**, 1033–1034.
- (93) Wada, S.; Suzuki, H. *Tetrahedron Lett.* **2003**, *44*, 399–401.
- (94) Smahi, A.; Solhy, A.; El Badaoui, H.; Amoukal, A.; Tikad, A.; Maizi, M.; Sebti, S. *Appl. Catal., A* **2003**, *250*, 151–159.
- (95) Reddy, T. I.; Varma, R. S. *Tetrahedron Lett.* **1997**, *38*, 1721–1724.
- (96) Saravananurugan, S.; Palanichamy, M.; Hartmann, M.; Murugesan, V. *Appl. Catal., A* **2006**, *298*, 8–15.
- (97) Aguado, S.; Canivet, J.; Farrusseng, D. *J. Mater. Chem.* **2011**, *21*, 7582.
- (98) Aguado, S.; Canivet, J.; Schuurman, Y.; Farrusseng, D. *J. Catal.* **2011**, *284*, 207.
- (99) Climent, M. J.; Corma, A.; Iborra, S.; Velty, A. *J. Mol. Catal. A: Chem.* **2002**, *182*–183, 327.
- (100) Boronat, M.; Climent, M. J.; Corma, A.; Iborra, S.; Monton, R.; Sabater, M. J. *Chem. - Eur. J.* **2010**, *16*, 1221.
- (101) Farrusseng, D.; Aguado, S.; Pinel, C. *Angew. Chem., Int. Ed.* **2009**, *48*, 7502.
- (102) Lempers, H. E. B.; Sheldon, R. A. *J. Catal.* **1998**, *175*, 62–69.

(103) Panchenko, V. N.; Matrosova, M. M.; Jeon, J.; Jun, J. W.; Timofeeva, M. N.; Jhung, S. H. *J. Catal.* **2014**, *316*, 251–259.